

## THE ROLE OF HeH<sup>+</sup> IN COOL HELIUM-RICH WHITE DWARFS

G. J. HARRIS, A. E. LYNAS-GRAY,<sup>1</sup> S. MILLER, AND J. TENNYSON<sup>2</sup>

Department of Physics and Astronomy, University College London, Gower Street, London WC1E 6BT, UK

Received 2004 October 11; accepted 2004 November 11; published 2004 November 19

### ABSTRACT

HeH<sup>+</sup> is found to be the dominant positive ion over a wide range of temperatures and densities relevant to helium-rich white dwarfs. The inclusion of HeH<sup>+</sup> in ionization equilibrium computations increases the abundance of free electrons by a significant factor. For temperatures below 8000 K, He<sup>-</sup> free-free absorption is increased by up to a factor of 5 by the inclusion of HeH<sup>+</sup>. Illustrative model atmospheres and spectral energy distributions are computed, which show that HeH<sup>+</sup> has a strong effect on the density and pressure structure of helium-rich white dwarfs with  $T_{\text{eff}} < 8000$  K. The inclusion of HeH<sup>+</sup> significantly reddens spectral energy distributions and broadband color indices for models with  $T_{\text{eff}} < 5500$  K. This has serious implications for existing model atmospheres, synthetic spectra, and cooling curves for helium-rich white dwarfs.

*Subject headings:* equation of state — stars: atmospheres — white dwarfs

### 1. INTRODUCTION

Bergeron & Leggett (2002) analyzed the recently discovered white dwarfs SDSS J133739+000142 and LHS 3250 (Harris et al. 1999 2001), identifying both objects as extreme helium-rich cool white dwarfs. However, they encountered significant problems when attempting to fit the spectral energy distributions (SEDs). Bergeron & Leggett (2002) concluded that the discrepancy between their SEDs and the observed fluxes is due to the physics used to calculate their model atmospheres. Here we investigate the molecular ion HeH<sup>+</sup> as part of the missing physics of helium-rich white dwarfs. We demonstrate that the opacity of a helium-rich white dwarf’s photosphere is significantly affected by HeH<sup>+</sup>. From the discussion of Fontaine et al. (2001), it follows that increased opacity arising from HeH<sup>+</sup> will lengthen the cooling time for helium-rich white dwarfs with  $T_{\text{eff}} < 8000$  K.

The only attempt to study HeH<sup>+</sup> in helium-rich white dwarfs known to us was made by Gaur et al. (1988 1992). They showed that HeH<sup>+</sup> exists in significant quantities in helium-rich white dwarfs and suggested a search for the infrared lines of HeH<sup>+</sup>.

### 2. EQUATION OF STATE

The equation of state (EOS) is a vital component of any model atmosphere; it links the state parameters such as temperature, pressure, density, and internal energy. It also calculates the relative abundance of each species within the gas, which is essential to obtain accurate radiative opacities. The photospheres of cool, extremely helium-rich white dwarfs have densities that can reach upward of  $1 \text{ g cm}^{-3}$ ; under such conditions the use of a nonideal EOS is required.

We have adapted the nonideal H/He EOS of Luo (1997). This EOS accounts for the nonideal effects of electron degeneracy, Coulomb coupling, and pressure ionization but lacks an accurate treatment of pressure dissociation. The abundance of H<sub>2</sub> is estimated using an equilibrium constant for the reaction: H<sub>2</sub> ⇌ 2H, so that H<sub>2</sub> pressure dissociates as hydrogen pressure ionizes.

To account for the pressure ionization of H<sup>-</sup>, we have added

a term to the hydrogen ionization equilibrium, given by equations (22) and (23) in Luo (1997), so that

$$\begin{aligned} y_{\text{H}^-} &= L_{\text{H}^-}/L_{\text{H}}, \\ L_{\text{H}} &= L_{\text{H}_1} + L_{\text{H}_{\text{II}}} + L_{\text{H}^-}, \end{aligned} \quad (1)$$

where  $y_{\text{H}^-}$  is the ionization fraction of atomic and ionic hydrogen in the form of H<sup>-</sup>, and  $L_{\text{H}_1}$  and  $L_{\text{H}_{\text{II}}}$  are the grand partition functions of atomic hydrogen and a proton (see Luo 1997, eq. [23]). The grand partition function of H<sup>-</sup> is given by

$$L_{\text{H}^-} = W_{\text{H}^-} \exp(2\lambda - E_{\text{H}^-}/kT), \quad (2)$$

where  $\lambda$  is the electron degeneracy,  $E_{\text{H}^-}$  is the sum of the ionization potential of hydrogen and H<sup>-</sup> (14.352 eV), and  $W_{\text{H}^-}$  is given by equations (11)–(16) in Luo (1997) using a characteristic radius for H<sup>-</sup> of 1.15 Å (Lenzuni & Saumon 1992).

Under certain conditions, the trace ionic molecules H<sub>2</sub><sup>-</sup>, H<sub>2</sub><sup>+</sup>, H<sub>3</sub><sup>+</sup>, HeH<sup>+</sup>, and He<sub>2</sub><sup>+</sup> are responsible for nearly all the free electrons in a H/He gas. We calculate equilibrium constants for the formation of H<sub>2</sub>, H<sub>2</sub><sup>-</sup>, H<sub>2</sub><sup>+</sup>, H<sub>3</sub><sup>+</sup>, HeH<sup>+</sup>, and He<sub>2</sub><sup>+</sup> from atomic H and He, H<sup>-</sup>, and free electrons with the Saha equation. Subject to conservation of charge and of H and He nuclei, the equilibrium constants and ionization fractions are used to construct three nonlinear simultaneous equations. These three equations are solved using a multivariable Newton-Raphson technique. In this way the number densities for each species can be calculated for any given temperature, pressure, hydrogen fraction, and value of  $\lambda$ . The internal partition functions that we use are detailed in Harris et al. (2004); for HeH<sup>+</sup> we use the partition function of Engel et al. (2004). A converged value of  $\lambda$  is found by iterating over a further conservation of charge equation:

$$\begin{aligned} C_e T^{3/2} F_{1/2}(\lambda - \epsilon_{\text{CC}}/kT) &= N_{\text{H}_{\text{II}}} + N_{\text{He}_{\text{II}}} + 2N_{\text{He}_{\text{III}}} - N_{\text{H}^-} + N_{\text{H}_2^+} \\ &\quad - N_{\text{H}_2^-} + N_{\text{H}_3^+} + N_{\text{HeH}^+} + N_{\text{He}_2^+}, \end{aligned} \quad (3)$$

where  $N_x$  is the number density of species  $x$ ,  $\epsilon_{\text{CC}}$  is the free electron Coulomb coupling energy (Luo 1997),  $F_{1/2}$  is a Fermi-Dirac integral,  $T$  is temperature, and a constant  $C_e$  =

<sup>1</sup> Permanent address: Department of Physics, University of Oxford, Keble Road, Oxford OX1 3RH, UK.

<sup>2</sup> Corresponding author; j.tennyson@ucl.ac.uk.

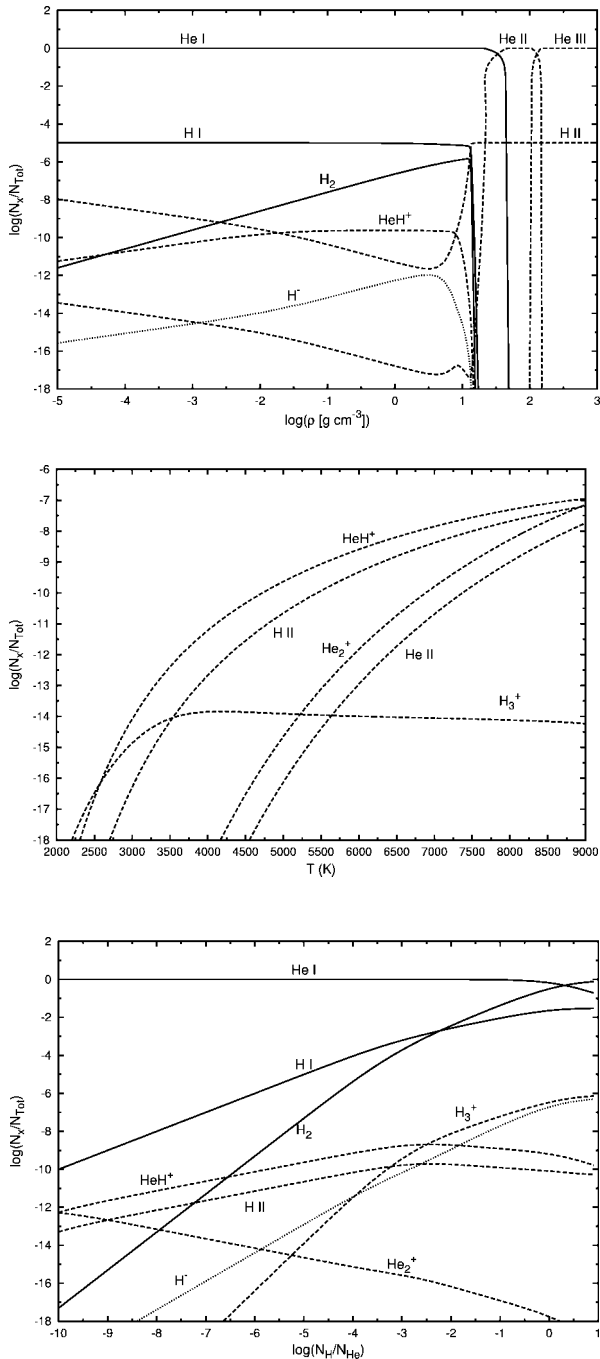


FIG. 1.—Chemical and ionization equilibrium as a function of  $\log(N_{\text{H}}/N_{\text{He}})$ , density, and temperature. Values of temperature of 5000 K, density of  $0.2 \text{ g cm}^{-3}$ , and  $\log(N_{\text{H}}/N_{\text{He}}) = -5$  are used. Neutral species are given solid lines, positively charged species dashed lines, and negatively charged species dotted lines.

$(2^{1/2}/\pi^2)(km_e/\hbar^2)^{3/2}$ . The left-hand side of equation (3) is the number density of free electrons (see Luo 1994 1997), and the right-hand side counts the charge on all ions.

Figure 1 shows the number fraction of the species within our EOS, as a function of H-to-He number ratio, density, and temperature. At 5000 K and density of  $0.2 \text{ g cm}^{-3}$ ,  $\text{H}_3^+$  is the dominant positive ion for the hydrogen-rich case.  $\text{HeH}^+$  is the dominant positive ion for the helium-rich range  $-10 < \log(N_{\text{H}}/N_{\text{He}}) < -2.5$ , and  $\text{He}_2^+$  becomes the dominant positive ion for  $\log(N_{\text{H}}/N_{\text{He}}) < -10$ . Figure 1 indicates that  $\text{HeH}^+$  continues to be the dominant positive ion over a range of densities and tem-

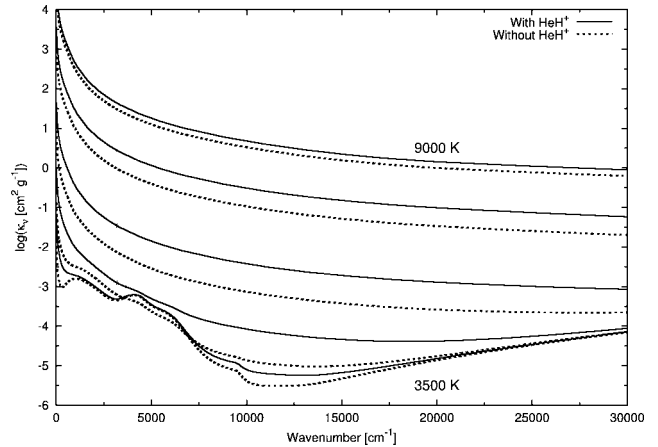


FIG. 2.—Continuous opacity function as a function of wavenumber at constant values of  $\rho = 0.5 \text{ g cm}^{-3}$  and  $\log(N_{\text{H}}/N_{\text{He}}) = -5$ , calculated at temperatures of 9000, 7000, 5000, 4000, and 3500 K.

peratures. Lenzuni et al. (1991) present an EOS and mean opacities for a H/He gas of 72% hydrogen by mass. They correctly state that the opacity coefficient of  $\text{HeH}^+$  is wholly irrelevant. However, as illustrated below, for a helium-rich mix  $\text{HeH}^+$  strongly affects the opacity and cannot be neglected.

### 3. OPACITY FUNCTION

The opacity of a gas under the extreme pressures found in the photospheres of helium-rich white dwarfs remains in question (Iglesias et al. 2002; Bergeron & Leggett 2002). The opacity of a cool helium-rich atmosphere is dominated by  $\text{H}_2$ -He collision-induced absorption,  $\text{He}^-$  free-free absorption, and He I Rayleigh scattering (Malo et al. 1999; Iglesias et al. 2002; Rohrmann et al. 2002). As such, the opacity is strongly dependent on the abundance of free electrons and  $\text{H}_2$ . The sources of opacity data that we use are discussed in Harris et al. (2004).

The monochromatic absorption coefficient at  $\rho = 0.5 \text{ g cm}^{-3}$ ,  $\log(N_{\text{H}}/N_{\text{He}}) = -5$ , over a range of temperatures, computed both including and neglecting  $\text{HeH}^+$  from our EOS, is shown in Figure 2. It is evident that if  $\text{HeH}^+$  is neglected, the gas opacity can be underestimated by as much as a factor of 5 over a significant range of temperatures. The dominant opacity, across the frequency range shown in Figure 2 and for temperatures upward of 5000 K, is  $\text{He}^-$  free-free absorption. At lower temperatures, collision-induced absorption in the infrared and He I Rayleigh scattering in the visible/ultraviolet become important and eventually take over from  $\text{He}^-$  free-free.

To determine if  $\text{HeH}^+$  rotation-vibration lines would be observable in a helium-rich white dwarf, we have employed the recent publicly available  $\text{HeH}^+$  line list of Engel et al. (2004). We find that the absorption lines of  $\text{HeH}^+$  are too weak to overcome the continuous opacity, under the temperatures and densities found in helium-rich white dwarfs. Therefore,  $\text{HeH}^+$  lines will not be visible in the spectra of helium-rich white dwarfs. For a discussion of  $\text{HeH}^+$  line opacity and some of the temperature densities in which it is important, see Engel et al. (2004).

### 4. MODEL ATMOSPHERES AND SPECTRAL ENERGY DISTRIBUTIONS

We use the plane-parallel model atmosphere code MARCS (Gustafsson et al. 1975), modified for the new nonideal EOS subroutines discussed in § 2 and the new continuous opacity

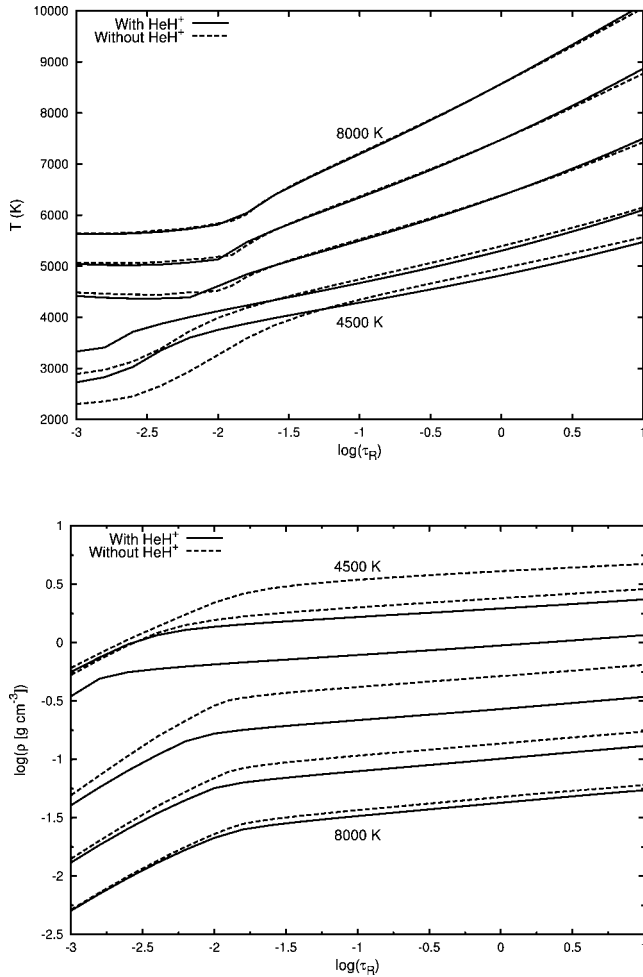


FIG. 3.—Optical depth vs. temperature and density for models of 4500, 5000, 6000, 7000, and 8000 K, computed including and neglecting HeH<sup>+</sup> in the ionization equilibrium, with  $\log(N_{\text{H}}/N_{\text{He}}) = -5$ .

subroutines discussed in § 3. The new EOS and opacity function subroutines are fast enough to be run in real time.

As discussed in Saumon et al. (1994) and Bergeron et al. (1995), in the optically thin regions, the unusual opacity function of a metal-free H/He gas results in multiple roots in the equation of radiative equilibrium. The high-temperature solution to radiative equilibrium in the optically thin regions is

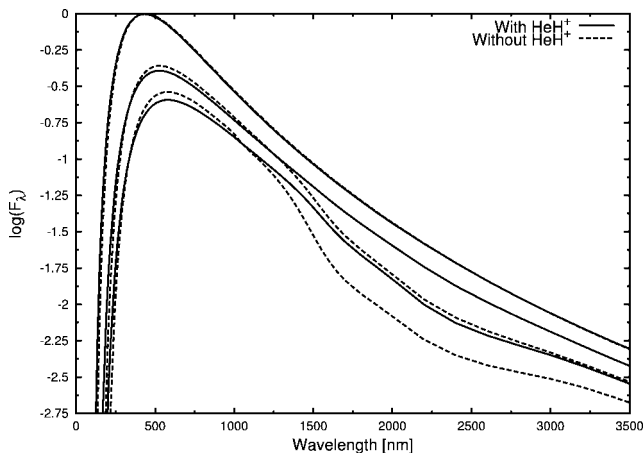


FIG. 4.—SEDs for models of  $T_{\text{eff}} = 4500, 5000,$  and  $6000$  K. The logarithm of the relative flux is given per unit wavelength interval.

TABLE 1

COLOR INDICES FOR MODELS CALCULATED WHILE NEGLECTING HeH<sup>+</sup>

$T_{\text{eff}}$	$B - V$	$V - R$	$V - K$	$R - I$	$I - J$	$J - H$	$H - K$
4500 .....	0.85	0.52	0.58	0.48	0.30	-0.54	-0.17
5000 .....	0.72	0.44	0.81	0.42	0.35	-0.18	-0.22
5500 .....	0.60	0.38	1.14	0.36	0.32	0.12	-0.04
6000 .....	0.50	0.32	0.98	0.30	0.24	0.12	-0.01
6500 .....	0.42	0.27	0.77	0.25	0.18	0.09	-0.03
7000 .....	0.36	0.23	0.59	0.21	0.12	0.07	-0.05
7500 .....	0.30	0.20	0.43	0.17	0.07	0.05	-0.06
8000 .....	0.25	0.17	0.30	0.14	0.03	0.03	-0.08

NOTE.—Here  $\log g = 8$ , and  $\log(N_{\text{H}}/N_{\text{He}}) = 10^{-5}$ .

preferentially found in our models. Such a solution is not physically realistic, rendering our models of  $T_{\text{eff}} \leq 5000$  K below  $\log \tau_R = -2$  unreliable. However, as this only occurs at very small optical depths, the emergent flux is unaffected.

We also experienced a problem with convergence of the convective flux at temperatures of 5000 K and below. The pressure-temperature gradient ( $\nabla$ ) is very close to the adiabatic gradient ( $\nabla_{\text{ad}}$ ), so that  $(\nabla - \nabla_{\text{ad}})/\nabla \sim 10^{-3}$  in the convective zone. In the cool, highly nonideal regions, numerical noise in the value of  $\nabla_{\text{ad}}$  calculated within our EOS is of this order, resulting in convergence problems with the convective flux. We have therefore not been able to obtain converged models below  $T_{\text{eff}} = 4500$  K.

We have computed a set of model atmospheres for  $\log g = 8$ ,  $\log(N_{\text{H}}/N_{\text{He}}) = 10^{-5}$ , and between effective temperatures of 4500 and 8000 K, including and neglecting HeH<sup>+</sup>. Figure 3 shows optical depth versus temperature and density for model atmospheres of 4500, 5000, 6000, 7000, and 8000 K. Although the temperatures remain relatively unperturbed by the inclusion of HeH<sup>+</sup>, there is a very strong effect on the density and pressure. If HeH<sup>+</sup> is neglected, then the density and pressure can be overestimated by up to a factor of 5; similarly, the electron pressure can be significantly underestimated. For  $T_{\text{eff}}$  of  $\geq 8000$  K there are significant numbers of electrons released from H II and He II, which reduces the importance of HeH<sup>+</sup>.

Figure 4 shows the SEDs of our 4500, 5000, and 6000 K models, with and without HeH<sup>+</sup>. The 4500 and 5000 K SEDs show significant changes if HeH<sup>+</sup> is included in the ionization equilibrium, but the effect is only small for the 6000 K model. The reason for this is that above  $\sim 5000$  K, He<sup>-</sup> free-free is the only significant source of opacity, so although the total opacity is increased the shape of the absorption function and hence SED is unchanged. For temperatures below 5500 K, He Rayleigh scattering and He-H<sub>2</sub> collision-induced absorption contribute to opacity. As these opacity sources are unaffected by the increased abundance of electrons from HeH<sup>+</sup>, the increase in He<sup>-</sup> free-free opacity changes the shape of the total opacity function and SED. These differences are reflected in the broadband color indexes given in Tables 1 and 2. These colors were computed by using the bandpasses given by Bessel & Brett

TABLE 2

COLOR INDICES FOR MODELS CALCULATED WITH HeH<sup>+</sup>

$T_{\text{eff}}$	$B - V$	$V - R$	$V - K$	$R - I$	$I - J$	$J - H$	$H - K$
4500 .....	0.84	0.52	1.32	0.51	0.49	-0.03	-0.18
5000 .....	0.70	0.44	1.44	0.43	0.42	0.16	-0.01
5500 .....	0.59	0.37	1.23	0.36	0.32	0.16	0.02
6000 .....	0.50	0.32	0.98	0.30	0.24	0.13	0.00
6500 .....	0.42	0.27	0.80	0.25	0.18	0.10	-0.03
7000 .....	0.35	0.23	0.59	0.21	0.12	0.07	-0.04
7500 .....	0.30	0.20	0.43	0.17	0.07	0.05	-0.06
8000 .....	0.25	0.17	0.29	0.14	0.03	0.03	-0.08

NOTE.—Here  $\log g = 8$ , and  $\log(N_{\text{H}}/N_{\text{He}}) = 10^{-5}$ .

(1988) and Bessel (1990) and calibrating using a spectrum of Vega. There are significant differences, at  $T_{\text{eff}} = 5500$  K and below, between colors computed while including and neglecting  $\text{HeH}^+$ . The large increase in the  $V - K$  magnitude and most of the other color indices indicates that the models calculated with  $\text{HeH}^+$  are significantly redder than the models calculated without  $\text{HeH}^+$ . This is also apparent in the SEDs. In general, all our colors are redder than the colors of Bergeron & Leggett (2002).

## 5. CONCLUSION

A nonideal H/He EOS that includes the molecular ion  $\text{HeH}^+$  within the ionization equilibrium has been presented. It has been demonstrated that under helium-rich conditions and over a range of temperatures and densities relevant to helium-rich white dwarfs,  $\text{HeH}^+$  is the dominant positive ion. Using the EOS, we have computed a set of continuous opacities that illustrate that  $\text{HeH}^+$  can indirectly increase the opacity of a helium-rich gas by up to a factor of 5. Using the recent  $\text{HeH}^+$  line list of Engel et al. (2004), we have found that  $\text{HeH}^+$  line opacity does not significantly contribute to the opacity at the densities found in helium-rich white dwarfs.

From a physical point of view, one of the most interesting reasons for studying helium-rich white dwarfs is that the den-

sities of their photospheres access regions in which the gas is strongly nonideal. Saumon & Chabrier (1991) and Saumon et al. (1995) have studied the pressure dissociation of  $\text{H}_2$  in a pure hydrogen environment. However, one of the shortcomings of our EOS and all other EOSs known to us is that there has been no study of the pressure dissociation of the important molecular ions,  $\text{H}_3^+$ ,  $\text{HeH}^+$ , and  $\text{He}_2^+$ . Before we can fully understand helium-rich white dwarfs, our understanding of the physics of cool dense H/He plasmas must be improved.

Our EOS and opacity function has been incorporated into a version of MARCS (Gustafsson et al. 1975). Using this code, we have computed model atmospheres, SEDs, and broadband color indices for an illustrative range of helium-rich white dwarfs. We find that in all models below 8000 K, the pressure and density of the model atmospheres is reduced by up to a factor of 5 by the inclusion of  $\text{HeH}^+$ . Furthermore,  $\text{HeH}^+$  significantly reddens the SEDs and color indices for models below  $T_{\text{eff}} = 5500$  K. The importance of  $\text{HeH}^+$  should prompt a review of all current model atmospheres, synthetic spectra, and cooling curves for cool helium-rich white dwarfs.

We thank Professor Bengt Gustafsson for providing us with a version of MARCS, Professor Hugh Jones for providing a spectrum of Vega, and the UK Particle Physics and Astronomy Research Council for support.

## REFERENCES

- Bergeron, P., & Leggett, S. K. 2002, *ApJ*, 580, 1070  
 Bergeron, P., Saumon, D., & Wesemael, F. 1995, *ApJ*, 443, 764  
 Bessel, M. S. 1990, *PASP*, 102, 1181  
 Bessel, M. S., & Brett, J. M. 1988, *PASP*, 100, 1134  
 Engel, E. A., Doss, N., Harris, G. J., & Tennyson, J. 2004, *MNRAS*, in press (astro-ph/0411267)  
 Fontaine, G., Brassard, P., & Bergeron, P. 2001, *PASP*, 113, 409  
 Gaur, V. P., Joshi, G. C., & Pande, M. C. 1992, *Ap&SS*, 197, 57  
 Gaur, V. P., Tripathi, G. C., Joshi, G. C., & Pande, M. C. 1988, *Ap&SS*, 147, 107  
 Gustafsson, B., Bell, R. A., Eriksson, K., & Nordlund, Å. 1975, *A&A*, 42, 407  
 Harris, G. J., Lynas-Gray, A. E., Miller, S., & Tennyson, J. 2004, *ApJ*, 600, 1025  
 Harris, H. C., Dahn, C. C., Vrba, F. J., Henden, A. A., Liebert, J., Schmidt, G. D., & Reid, I. N. 1999, *ApJ*, 524, 1000  
 Harris, H. C., et al. 2001, *ApJ*, 549, L109  
 Iglesias, C. A., Rogers, F. J., & Saumon, D. 2002, *ApJ*, 569, L111  
 Lenzuni, P., Chernoff, D. F., & Salpeter, E. E. 1991, *ApJS*, 76, 759  
 Lenzuni, P., & Saumon, D. 1992, *Rev. Mexicana Astron. Astrofis.*, 23, 223  
 Luo, G. Q. 1994, *A&A*, 281, 460  
 ———. 1997, *ApJ*, 491, 366  
 Malo, A., Wesemael, F., & Bergeron, P. 1999, *ApJ*, 517, 901  
 Rohrmann, R. D., Serenelli, A. M., Althaus, L. G., & Benvenuto, O. G. 2002, *MNRAS*, 335, 499  
 Saumon, D., Bergeron, B., Lunine, J. I., Hubbard, W. B., & Burrows, A. 1994, *ApJ*, 424, 333  
 Saumon, D., & Chabrier, G. 1991, *Phys. Rev. A*, 44, 5122  
 Saumon, D., Chabrier, G., & Van Horn, H. M. 1995, *ApJS*, 99, 713